

Dimension dependent energy thresholds for discrete breathers

Michael Kastner†

† Physikalisches Institut, Lehrstuhl für Theoretische Physik I, Universität Bayreuth,
95440 Bayreuth, Germany

E-mail: Michael.Kastner@uni-bayreuth.de

Abstract. Discrete breathers are time-periodic, spatially localized solutions of the equations of motion for a system of classical degrees of freedom interacting on a lattice. We study the existence of energy thresholds for discrete breathers, i.e., the question whether, in a certain system, discrete breathers of arbitrarily low energy exist, or a threshold has to be overcome in order to excite a discrete breather. Breather energies are found to have a positive lower bound if the lattice dimension d is greater than or equal to a certain critical value d_c , whereas no energy threshold is observed for $d < d_c$. The critical dimension d_c is system dependent and can be computed explicitly, taking on values between zero and infinity. Three classes of Hamiltonian systems are distinguished, being characterized by different mechanisms effecting the existence (or non-existence) of an energy threshold.

PACS numbers: 45.05.+x, 63.20.Pw, 05.45.-a

1. Introduction

Discrete breathers are time-periodic, spatially localized solutions of the equations of motion for a system of classical degrees of freedom interacting on a lattice. They are also called *intrinsically localized*, in distinction to Anderson localization triggered by disorder. A necessary condition for their existence is the nonlinearity of the equations of motion of the system, and the existence of discrete breathers has been proved rigorously for some classes of systems [1, 2, 3, 4, 5, 6, 7]. In contrast to their analogues in continuous systems, the existence of discrete breathers is a generic phenomenon, which accounts for considerable interest in these objects from a physical point of view in the last decade. In fact, recent experiments could demonstrate the existence of discrete breathers in various real systems such as low-dimensional crystals [8], antiferromagnetic materials [9], Josephson junction arrays [10, 11], molecular crystals [12], coupled optical waveguides [13], and micromechanical cantilever arrays [14].

Properties of discrete breathers, as well as of some generalizations of discrete breathers, have been studied in detail in a large variety of different models. However, apart from existence proofs and studies of the spatial localization of discrete breathers

(which is typically exponential), only a few general results exist. Among these it is worth mentioning the remarkable result by Flach, Kladko, and MacKay [15] on energy thresholds for discrete breathers in one-, two-, and three-dimensional lattices (and subsequent generalizations to systems with long range interactions [16] and to partially isochronous potentials [17]). Results on energy thresholds have practical relevance, as they can assist in choosing a proper energy range for the detection of discrete breathers in real experiments or computer experiments. It is found that, for Hamiltonian systems of infinite size, energy thresholds depend on the spatial dimension d of the system. A critical spatial dimension d_c exists, such that

- for a system whose spatial dimension d is smaller than d_c , discrete breathers of arbitrarily low energy can be found, i.e., no energy threshold exist,
- for a system where $d \geq d_c$, an energy threshold exists, i.e., there is a positive lower bound on the energy of discrete breathers.

The existence or absence of an energy threshold for discrete breathers beautifully explains certain observations made in discrete systems. One example are statistical properties characterizing the spontaneous formation of discrete breathers in cooled lattices [18], a second example are the power spectra observed in thermalized lattices [19]. In both cases, the presence of an energy threshold induces a qualitative change in the quantities under investigation.

The result on energy thresholds in [15] was derived under assumptions which turned out to be not general enough to cover all classes of systems of physical interest, and neither all of the different mechanisms leading to the (non)existence of an energy threshold. In this article, a much richer scenario is described, taking into account a larger class of systems and, most notably, pointing out three different mechanisms effecting the existence (or non-existence) of an energy threshold. The conditions leading to the occurrence of any of these mechanisms will be worked out, providing means to predict the existence of energy thresholds. A flavour of at least a part of these results has been given previously in a letter [20]. In the present article, a more general situation is considered and details and derivations are given.

There are three additional classes of systems, not covered in [15], for which energy thresholds and critical dimensions are discussed in the present article: Firstly, systems with nonanalytic potential are included in the analysis. Albeit rare, physical systems with such interactions exist and are under experimental investigation, for example in the field of granular media [21]. Secondly, systems in which no low amplitude discrete breathers exist are considered. Even for the class of systems with analytic potentials, these systems constitute a generic subclass, which accounts for their possible relevance in physics. Thirdly, results indicating the absence of an energy threshold in systems with no linear spectrum are presented. These kind of systems have attracted much interest recently, and strongly nonlinear tunable phononic crystals showing such a behaviour are currently being constructed [22].

The article is organized as follows: in section 2 some notation is fixed, defining the

classes of systems under consideration. Then, it is appropriate to distinguish between systems *with* and *without* a linear spectrum. Section 3 is devoted to the first category, and the existence of an energy threshold is traced back to the occurrence of a certain modulational instability. Systems without a linear spectrum are treated in section 4. Finally, in section 5, the results for the various cases are summarized, providing a compilation of the different mechanisms which effect the existence of an energy threshold and specifying the conditions which give rise to each of these mechanisms.

2. Equations of motion

We consider a hypercubic lattice $\mathcal{L}_d = \{1, \dots, L\}^d$ in $d \in \mathbb{N}$ spatial dimensions. For simplicity, we consider $L \in 2\mathbb{Z}$ an even number. Each of the $N = L^d$ sites is labelled by a d -dimensional vector $n \in \mathcal{L}_d$, and to each site a state (p_n, x_n) is assigned, where both, the momenta $p_n \in \mathbb{R}^f$ and the positions $x_n \in \mathbb{R}^f$, are vectors of a finite number f of components. The dynamical properties of the system are governed by the Hamiltonian function

$$H = \sum_{n \in \mathcal{L}_d} \left[\frac{p_n^2}{2} + V(x_n) + \sum_{m \in \mathcal{N}_n} W(x_m - x_n) \right] \quad (1)$$

with periodic boundary conditions in all spatial directions. V is called on-site potential, $W \neq 0$ interaction potential, and site n is assumed to interact with its neighbourhood \mathcal{N}_n of nearest neighbouring sites on the lattice.

The potentials V and W are both assumed to attain minima for zero argument, and, without loss of generality, $V(0) = 0$ and $W(0) = 0$. In contrast to previous related work [23, 15, 17], analyticity (in the sense of the existence of a Taylor series) of the potentials around their minima is not required. By removing this restriction of analyticity, additional models of physical interest are included, as for example granular media are described by means of nonanalytic interaction potentials [21].

Several of the above restrictions on the system are imposed only for notational simplicity of what follows. Extending the computations to systems of different lattice geometries or interactions not only with nearest neighbours should be possible without any substantial change and are discussed to some extend in section 3.8. The case of long-range interactions is not included in the following analysis. A treatment of such systems can be found in [16], and these results will be confronted with those for short-range interactions in section 3.8.

For the sake of readability, analytic calculations will be performed for the one-dimensional case

$$H = \sum_{n=1}^N \left[\frac{p_n^2}{2} + V(x_n) + W(x_{n+1} - x_n) \right], \quad (2)$$

again with periodic boundary conditions $p_{n+N} = p_n$ and $x_{n+N} = x_n$, where momenta as well as positions are assumed to be one-component ($f = 1$). The effect of the dimensionality on the results will be discussed in section 3.4.

The existence of an energy threshold for discrete breathers will depend on the asymptotic behaviour of the potentials V and W close to their minima, and therefore we choose to represent V and W as power series in their arguments,

$$V(x) = \sum_{\mu=0}^{\infty} \frac{v_{\mu}}{r_{\mu}} |x|^{r_{\mu}}, \quad W(x) = \sum_{\mu=0}^{\infty} \frac{\phi_{\mu}}{r_{\mu}} |x|^{r_{\mu}}, \quad (3)$$

with real (but not necessarily integer) exponents $r_{\mu} \geq 1$. For convenience we consider the powers to be of increasing order, $r_{\mu} < r_{\mu+1}$ for all μ . Some of the coefficients v_{μ} and/or ϕ_{μ} may be zero, and in this way the expansions in (3) can also account for potentials V and W having different powers. Note that, by treating this class of potentials, we will be able to make statements about energy thresholds for the even larger class of potentials which have (3) as expansions around their minima. The potentials V and W in (3) are chosen to be symmetric, and this restriction is made to keep the calculations simpler and the presentation more readable, as the number of cases to be distinguished is reduced in this way. For systems with linear spectrum and in the case of analytic potentials, the analysis of systems with asymmetric potentials can be found in [23]. These results, as well as the possibility of a generalization of our results to more general systems with asymmetric potentials, are briefly discussed in section 3.8.

The equations of motion following from (2) are

$$\ddot{x}_n + V'(x_n) + W'(x_n - x_{n-1}) - W'(x_{n+1} - x_n) = 0, \quad (4)$$

where a dot denotes a total derivative with respect to time, a prime the derivative of a function with respect to its argument. It is convenient to introduce a transform to normal coordinates

$$Q_q = \frac{1}{N} \sum_{n=1}^N e^{iqn} x_n, \quad q = \frac{2\pi l}{N}, \quad l \in \left\{ -\frac{N}{2} + 1, \dots, \frac{N}{2} \right\}, \quad (5)$$

where the inverse transform is given by

$$x_n = \sum_q e^{-iqn} Q_q. \quad (6)$$

The normal coordinates $Q_q(t)$, like the original ones $x_n(t)$, are functions of time, but this dependence will often be suppressed in the following. Rewriting the equations of motion (4) in terms of normal coordinates (5) yields

$$\ddot{Q}_q + F_q(Q) = 0, \quad (7)$$

where

$$F_q(Q) = \frac{1}{N} \sum_{n=1}^N e^{iqn} \left[V' \left(\sum_{q'} e^{-iq'n} Q_{q'} \right) + W' \left(\sum_{q'} (1 - e^{iq'}) e^{-iq'n} Q_{q'} \right) - W' \left(\sum_{q'} (e^{-iq'} - 1) e^{-iq'n} Q_{q'} \right) \right] \quad (8)$$

and Q denotes a vector with entries Q_q .

3. Systems with linear spectrum

In this section, we want to refer to systems with interaction potential $W(x) = \frac{\phi_0}{2}x^2 + \mathcal{O}(x^s)$ quadratic in leading order, i.e., $\phi_0 \neq 0$ and $s > 2$. (\mathcal{O} denotes Landau's order symbol.) The on-site potential, in contrast, can be either zero ($V = 0$), or of quadratic or higher order, $V(x) = \mathcal{O}(x^r)$ with $r \geq 2$. In the notation of the expansions in (3) this means $r_0 = 2$ and $\phi_0 \neq 0$. This setting of parameters allows linearization of the equations of motion (4) with a non-trivial result,

$$\ddot{Q}_q + \omega_q^2 Q_q = 0, \quad (9)$$

where

$$\omega_q^2 = v_0 + 4\phi_0 \sin^2\left(\frac{q}{2}\right) \quad (10)$$

denotes the frequency of the linear mode q . The set of all the ω_q^2 is called the linear spectrum. The differential equations (9) obviously decouple, having simple sine waves as solutions. In the following we will be interested in solutions of the *nonlinear* equations of motion (4) in the limit of small oscillation amplitudes in which the linearized equations of motion (9) are approached.

3.1. Main ideas of this section

For generic Hamiltonian systems, discrete breathers, like all periodic orbits, occur in one-parameter families. Some typical choices of quantities to index such a family are the energy of a discrete breather, its frequency, or its amplitude measured at the site of maximum amplitude. In numerical studies of discrete breathers in a variety of systems with linear spectrum, the following scenario has been observed: consider some discrete breather with frequency ω_{DB} outside the linear spectrum. When following the family of discrete breathers and approaching the edge ω_{edge} of the band formed by the frequencies of the linear spectrum, it may or may not be the case that the breather amplitude A goes to zero. The reverse conclusion, however, can be drawn: if discrete breathers of arbitrarily low amplitude exist, they cannot be found elsewhere but in the limit $\omega_{\text{DB}} \rightarrow \omega_{\text{edge}}$ [15]. Furthermore, in this case where

$$\lim_{\omega_{\text{DB}} \rightarrow \omega_{\text{edge}}} A_{\text{DB}}(\omega_{\text{DB}}) = 0, \quad (11)$$

it is observed numerically that in this limit the localization of the discrete breather becomes weaker and weaker. This fact is illustrated in figure 1, where, for the example of the a Fermi-Pasta-Ulam chain and discrete breathers of various frequencies, the maximum values of the amplitude are plotted for a number of lattice sites. More precisely, the localization strength approaches zero in the limit $\omega_{\text{DB}} \rightarrow \omega_{\text{edge}}$, and a transformation of a discrete breather into a spatially extended solution (plane wave) appears to take place. This observation gives rise to the following

HYPOTHESIS 1 *Consider a system with linear spectrum as specified above. Assume that in this system there exist low amplitude breathers, i.e., a family of discrete breathers for*

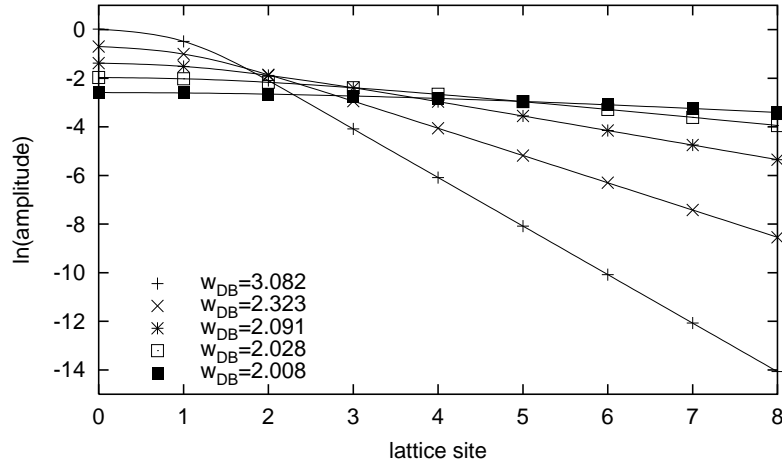


Figure 1. Shape profiles (maximum values of the amplitude) of discrete breathers, centered at lattice site 0, in a Fermi-Pasta-Ulam chain of $N = 99$ degrees of freedom (the equations of motion are given in (48) with parameter value $a = 0$). For a system which—like this one—has a linear spectrum, the localization is exponential (straight lines in the logarithmic plot). When the maximum breather amplitude is lowered (from $+$ to \blacksquare), the localization strength decreases and the solution attains more and more the shape of a plane wave. Lines are merely drawn to guide the eye.

which (11) holds. Then low amplitude breathers emerge from band edge plane waves by means of a tangent bifurcation.

A tangent bifurcation by definition takes place when a pair of Floquet multipliers of the linear stability analysis of the periodic orbit happens to collide at $+1$ on the unit circle. The periodic orbit emerging from the bifurcation appears to be of the same frequency as the one it originates from, and this is exactly the situation we observe for discrete breathers stemming from band edge modes.

The following three results or observations may serve to substantiate this hypothesis. Firstly, in a recent existence proof of discrete breathers due to James [6], it is shown for a large class of one-dimensional systems that discrete breathers of small amplitude exist and that they emerge from a bifurcation of a band edge plane wave. Secondly, Flach has shown in [23] that the periodic orbits emerging from the tangent bifurcation lack a certain permutation symmetry. This is consistent with the periodic orbits being discrete breathers, but inconsistent with plane wave-type solutions. Thirdly, to the knowledge of the author, in the numerous numerical studies of discrete breathers, there has never been observed a family of discrete breathers in a system with linear spectrum which, in the limit (if it exists) of the amplitude going to zero, is not subject to the attenuation of the localization strength as described above.

The above hypothesis allows to tackle the problem of the existence of an energy threshold for discrete breathers in the following way (which is the outline of the rest of this section): instead of directly treating discrete breathers, the analytically more easily accessible band edge plane waves are considered. Since it is the behaviour at low

amplitude which will be of importance, this can be done by employing perturbation techniques. Performing a Floquet analysis of these band edge plane waves, criteria for the appearance of a tangent bifurcation are found and the corresponding bifurcation energy is obtained. Then, the above hypothesis allows to relate this bifurcation energy to the energies of discrete breathers. In case the bifurcation energy is vanishing, no energy threshold is present. If the bifurcation energy is positive, an energy threshold has to be overcome in order to excite a discrete breather.

Note that there exist systems in which no low amplitude breathers are present and consequently the above hypothesis does not apply. This special case is deferred to section 3.9, whereas for the following sections we assume (11) to be valid.

3.2. Band edge modes

At the band edges of the linear spectrum, there exist two particularly simple periodic orbits Q^I and Q^{II} , each with only one mode excited,

$$\begin{aligned} \text{I: } Q_q &= 0 \quad \forall q \neq 0 \quad \text{and} \quad \ddot{Q}_0 + V'(Q_0) = 0, \\ \text{II: } Q_q &= 0 \quad \forall q \neq \pi \quad \text{and} \quad \ddot{Q}_\pi + V'(Q_\pi) + 2W'(2Q_\pi) = 0, \end{aligned} \quad (12)$$

where the excited mode is determined as the solution of the respective differential equation. Q^I is called the in-phase mode, characterized by identical oscillations at all sites, i.e., $x_{n+1}(t) = x_n(t)$ for all $n \in \{1, \dots, N\}$ at all times t . As is obvious from the differential equation for Q_0 in (12)I, the presence of an on-site potential V is essential for the existence of an in-phase mode. Q^{II} we will refer to as the out-of-phase mode, where each two neighbouring sites oscillate in opposition of phase, i.e., $x_{n+1}(t) = -x_n(t)$ for all $n \in \{1, \dots, N\}$ at all times t . Exemplarily, the following computations will be presented for the in-phase mode only.

Of a uniformly valid perturbative solution for the differential equation (12)I, for our purposes the leading term in the energy ε is sufficient,

$$Q_0(t) = \sqrt{\frac{2\varepsilon}{v_0}} \cos[\Omega(X)t + \varphi] + \text{h.o.t.}, \quad (13)$$

which can be obtained for example by means of a Lindstedt-Poincaré expansion [24] at low energy

$$\varepsilon(Q^I) = \frac{1}{2} \dot{Q}_0^2 + V(Q_0). \quad (14)$$

φ is an arbitrary phase shift which will be set to zero in the following, and higher order terms (h.o.t.) in the energy have been neglected. To render the expansion uniform, the nonlinear oscillation frequency

$$\Omega(X) = \sqrt{v_0} \left[1 + \frac{v_1}{v_0 \sqrt{\pi}} \frac{\Gamma(\frac{r_1+1}{2})}{\Gamma(\frac{r_1+2}{2})} X + \text{h.o.t.} \right] \quad (15)$$

has to be determined up to first order in

$$X = \left(\frac{2\varepsilon}{v_0} \right)^{(r_1-2)/2}, \quad (16)$$

where Γ is the Euler gamma function and higher order terms in X have been neglected. This series expansion can be derived either by standard perturbation techniques [24] or using a method put forward in [17].

3.3. Tangent bifurcation

Our aim is to determine the energy at which a band edge mode undergoes a tangent bifurcation. Such a bifurcation implies a pair of Floquet multipliers of the linear stability analysis of the periodic orbit to collide at $+1$ on the unit circle, and is hence accompanied by a change in stability. In order to investigate the stability properties of the band edge modes, a small perturbation is considered by substituting

$$Q_q \rightarrow Q_q + \delta_q \quad (17)$$

in the equations of motion (7). In the case of the periodic orbit Q^I , this substitution gives rise to equations of motions for the perturbations δ_q which, up to linear order in δ_q , read

$$\ddot{\delta}_q(t) + [\mathcal{V}''(t) + \omega_q^2] \delta_q(t) = 0, \quad (18)$$

where

$$\mathcal{V}''(t) = V''[Q_0(t)] - v_0, \quad (19)$$

and ω_q^2 is defined in (10). Note that this equation has a periodic coefficient \mathcal{V}'' , as Q_0 is a periodic function in time. This type of differential equation (ordinary, homogeneous, second order, with periodic coefficient) is termed Hill equation, and a number of theorems concerning stability are at hand. Let us briefly recall some properties of the Hill equation (for details see [25]) and outline how they can be exploited in order to determine the bifurcation energy.

It follows from Floquet theory that, depending on the values of the parameters present in (18), the Hill equation has either stable, unstable, or periodic solutions. Considering a suitable two-parameter space—in our case we choose the linear frequency ω_q and the energy ε , where the latter in turn determines \mathcal{V}'' —the regions of stable solutions display a particular shape in parameter space, the so-called Arnold tongues (see figure 11-3 in [24] for an illustration). Regions of stable solutions are separated from regions of unstable solutions by lines of periodic solutions. Hence, the parameter values at which the band edge mode Q^I bifurcates can be obtained by determining the values at which *any* of the δ_q has a periodic solution. The tangent bifurcation we are looking for appears at the smallest non-zero energy for which a periodic solution (13) of orbit I and a periodic solution of the corresponding variational equation (18), both with the same period, exist. In the following, by determining an energy expansion of the frequency $\tilde{\Omega}(\varepsilon)$ of the periodic solution of the variational equations (18), and equaling it with the frequency $\Omega(\varepsilon)$ of the periodic orbit (15), the bifurcation energy will be obtained to leading order.

The periodic solutions, as well as the corresponding parameter values, can be obtained by perturbation methods. In order to apply the Lindstedt-Poincaré technique [24], we introduce the transformation $\tau = \tilde{\Omega}(X)t$ into (18), yielding

$$\tilde{\Omega}^2(X)\ddot{\delta}_q(X, \tau) + [\mathcal{V}''(X, \tau) + \omega_q^2]\delta_q(X, \tau) = 0, \quad (20)$$

where a dot now denotes a total derivative with respect to τ . This change of variable transforms \mathcal{V}'' in a function which is π -periodic in τ . The energy dependence has been noted explicitly by the variable X . Inserting the Ansätze

$$\delta_q(X, \tau) = \delta_{q,0}(\tau) + \delta_{q,1}(\tau)X + \text{h.o.t.}, \quad (21)$$

$$\tilde{\Omega}^2(X) = \tilde{\Omega}_0^2 + \tilde{\Omega}_1^2 X + \text{h.o.t.}, \quad (22)$$

as well as the series expansions (13) and (15) in the Hill equation (20), terms of equal order in X can be collected to obtain the differential equations

$$\text{order } X^0 : \quad \tilde{\Omega}_0^2 \ddot{\delta}_{q,0}(\tau) + \omega_q^2 \delta_{q,0}(\tau) = 0, \quad (23)$$

$$\text{order } X^1 : \quad \tilde{\Omega}_0^2 \ddot{\delta}_{q,1}(\tau) + \omega_q^2 \delta_{q,1}(\tau) + \tilde{\Omega}_1^2 \ddot{\delta}_{q,0}(\tau) + \mathcal{V}_1''(\tau) \delta_{q,0}(\tau) = 0, \quad (24)$$

where the π -periodic function

$$\mathcal{V}_1''(\tau) = v_1(r_1 - 1) |\cos \tau|^{r_1-2} \quad (25)$$

has been defined. The solution of the zeroth order equation (23) is

$$\delta_{q,0}(\tau) = A \cos\left(\frac{\omega_q \tau}{\tilde{\Omega}_0}\right) + B \sin\left(\frac{\omega_q \tau}{\tilde{\Omega}_0}\right), \quad (26)$$

where A and B are complex valued constants. It follows from Floquet theory that, in order to obtain periodic solutions of period 2π of the first order equation (24) in the low energy limit, it is sufficient to consider only the first two terms of a Fourier series of the driving term,

$$\mathcal{V}_1''(\tau) = \sum_{k=0}^{\infty} C_k \cos(2k\tau) \quad (27)$$

with coefficients

$$C_0 = \frac{2v_1}{\sqrt{\pi}} \frac{\Gamma(\frac{r_1+1}{2})}{\Gamma(\frac{r_1}{2})}, \quad (28)$$

$$C_1 = 2^{2-r_1} \frac{v_1(r_1-2)\Gamma(r_1)}{\Gamma(\frac{r_1+2}{2})\Gamma(\frac{r_1}{2})}. \quad (29)$$

Inserting the truncated Fourier series as well as the zeroth order solution (26), the first order equation (24) reads

$$\tilde{\Omega}_0^2 \ddot{\delta}_{q,1}(\tau) + \omega_q^2 \delta_{q,1}(\tau) + [D + C_1 \cos(2\tau)] \delta_{q,0}(\tau) = 0, \quad (30)$$

where

$$D = C_0 - \left(\frac{\tilde{\Omega}_1 \omega_q}{\tilde{\Omega}_0}\right)^2. \quad (31)$$

The differential equation (30) is linear, and its solutions, which are in general aperiodic, can be obtained. Then, the periodic ones are found by eliminating the secular terms in the solution. This elimination is achieved only under certain conditions on the frequency, where the ones corresponding to the tangent bifurcation we are looking for are given by

$$\tilde{\Omega}_0^2 = \omega_q^2, \quad (32)$$

$$\tilde{\Omega}_1^2 = C_0 + \frac{C_1}{2}. \quad (33)$$

Equalling the truncated series expansions of the squared frequencies Ω^2 and $\tilde{\Omega}^2$, and solving for the variable X , the critical values

$$\varepsilon_{c,q}^I = \frac{v_0}{2} \left(\frac{v_0 - \omega_q^2}{C_1} \right)^{2/(r_1-2)} \quad (34)$$

of the energy at which a tangent bifurcation of orbit I may occur are obtained. Note that, in the preceding derivation of the bifurcation energy, we have simultaneously considered N uncoupled equations (18) for the perturbations δ_q , labelled by the index q . From δ_0 no bifurcation can arise, as this component simply effects a time shift of the periodic orbit [23]. A change of stability in any of the remaining equations, however, may give rise to a bifurcation. We are interested in the tangent bifurcation giving the lowest value of the bifurcation energy (34), which implies the choice $q = 2\pi/N$. For a large number of lattice sites N , we can write the corresponding linear frequency (10) as

$$\omega_{2\pi/N}^2 = v_0 + 4\pi^2 \phi_0 N^{-2} + \mathcal{O}(N^{-4}). \quad (35)$$

Inserting this expansion as well as equation (29), the bifurcation energy of orbit I reads

$$\varepsilon_c^I = \varepsilon_{c,2\pi/N}^I \simeq 2v_0 \left[\frac{\pi^2 \phi_0 r_1 \Gamma(\frac{r_1-2}{2}) \Gamma(\frac{r_1}{2})}{-N^2 v_1 \Gamma(r_1)} \right]^{2/(r_1-2)} \quad (36)$$

in leading order of N^{-1} . Since $v_0, \phi_0 > 0$ and since we have to demand a positive bifurcation energy, the tangent bifurcation can only occur if

$$v_1 < 0. \quad (37)$$

A similar analysis for the out-of-phase mode (periodic orbit II) yields the expression

$$\varepsilon_c^{II} \simeq \frac{v_0 + 4\phi_0}{2} \left[\frac{\pi^{5/2} \phi_0 r_1 \Gamma(\frac{r_1-2}{2})}{2N^2(v_1 + 2^{r_1} \phi_1) \Gamma(\frac{r_1+1}{2})} \right]^{2/(r_1-2)} \quad (38)$$

for the bifurcation energy. We have $v_0 \geq 0$ and $\phi_0 > 0$, leading to the necessary condition

$$v_1 + 2^{r_1} \phi_1 > 0 \quad (39)$$

for a tangent bifurcation to take place. Similar results in [23], derived for the case of analytic potentials V and W , are recovered by setting $r_1 = 4$. It was already noted in the same reference that conditions (37) and (39) mirror the fact that, for a tangent bifurcation to take place, it is necessary that the frequency of the band edge mode is repelled from the linear spectrum of the system with increasing energy.

3.4. Higher spatial dimensions

The computations and results of the preceding section can be generalized to systems of higher spatial dimensions d . The changes in the expressions of the bifurcation energies (36) and (38) are of small extent, and for our purposes it will only be important to note how the proportionality between the bifurcation energies ε_c and the system size N changes.

For arbitrary spatial dimension d , the normal coordinates (5) are labelled by a d dimensional vector $q = (q_1, \dots, q_d)$ with $q_i = \frac{2\pi l_i}{L}$ and $l_i \in \{-L/2 + 1, \dots, L/2\}$ for all i . Then, choosing the value of q giving rise to the lowest bifurcation energy, a factor $L^{4/(2-r_1)}$ is obtained in the expressions of the bifurcation energy instead of $N^{4/(2-r_1)}$. Since $N = L^d$, this is incorporated into (36) and (38) by replacing N by $N^{1/d}$. In this way for both, the in-phase as well as the out-of-phase mode, the proportionality

$$\varepsilon_c \propto N^{4/[d(2-r_1)]}, \quad (40)$$

connecting the bifurcation energy ε_c with the system size N , is obtained.

3.5. Energy thresholds for discrete breathers

The hypothesis of section 3.1 allows us to relate the bifurcation energy of the band edge plane wave to the minimum energy accessible for a discrete breather. It follows from (5) and (14) that the bifurcation energy determined above is an intensive quantity, i.e., on the scale of total energy per particle, and we will now turn to its extensive counterpart

$$E_c = N\varepsilon_c. \quad (41)$$

Considering the proportionality (40) in the limit of infinite system size $N \rightarrow \infty$, it is found that

$$\lim_{N \rightarrow \infty} E_c \propto \lim_{N \rightarrow \infty} N^{1-4/[d(r_1-2)]} \begin{cases} =0 & \text{if } d < d_c, \\ >0 & \text{if } d \geq d_c, \end{cases} \quad (42)$$

with critical dimension

$$d_c = \frac{4}{r_1-2}. \quad (43)$$

Hence, for systems of spatial dimension d smaller than the critical value d_c , discrete breathers of arbitrarily small energy can be found, whereas for systems where $d \geq d_c$ an energy threshold has to be overcome in order to excite a discrete breather. Equation (43) is in perfect agreement with the critical dimension $d_c = 2$ obtained in [15] for (generic) analytic potentials with a non-zero quadratic and quartic term, which, with our restriction to symmetric potentials, corresponds to a nonlinearity of leading order $r_1 = 4$.

This result for the critical dimension can be recovered by considering a continuum approximation of the discrete system as explained in [15]. In this approximation, the breather energy E_b can be expressed as an integral (equation (6) of reference [15]) which, in the limit of small breather amplitudes A , yields the proportionality $E_B \propto A^{(4-zd)/2}$.

For our choice of symmetric potentials V and W in (3), the detuning exponent z (see [15] for a definition) is equal to $r_1 - 2$. Then, considering E_b in the limit $A \rightarrow 0$, the expression (43) for the critical dimension d_c , distinguishing between finite and diverging limiting values for E_b , is reproduced.

3.6. Intuitive understanding

The mechanism which gives rise to an energy threshold for discrete breathers in high enough spatial dimension can be understood on an intuitive level. When lowering the amplitude of a discrete breather towards zero, two different mechanisms, competing with respect to their effect on the breather energy, take place: the localization strength of the discrete breather tends to become weaker, leading to an increase in energy, while the mere lowering in amplitude causes a decrease in energy (see figure 1 for an illustration). Depending on the respective strengths of these effects, an energy threshold may or may not exist. In the limit of weak localization, the degrees of freedom far from the breather's centre gain in importance. Their contribution to the energy depends on their 'number', which in turn depends on the spatial dimension of the system, and it is in this way that d enters the game.

3.7. Numerical confirmation of the results

Numerical computations have been performed in order to confirm the above result on energy thresholds for discrete breathers in systems with linear spectrum. By numerical continuation of periodic orbits from an anti-continuum limit [26], discrete breathers on finite lattices can be computed numerically up to machine precision. In particular, it is possible to continue a discrete breather along its family while varying a parameter. In doing so for a set of frequencies approaching the band edge of the linear spectrum, the dependence of the breather energy on its amplitude, measured at the site of maximum amplitude, can be determined. In order to test our main result, the existence or non-existence of an energy threshold of discrete breathers under certain conditions, we will confront such data for two exemplary systems, one displaying an energy threshold, the other not.

Consider a two-dimensional system ($d = 2$) of Fermi-Pasta-Ulam type, i.e., with zero on-site potential $V = 0$. The interaction potential W in the Hamiltonian (1) is chosen as

$$W(x) = \frac{1}{2}x^2 + \frac{1}{r_1}|x|^{r_1}, \quad (44)$$

giving rise to equations of motion of the form

$$\ddot{x}_n + \sum_{m \in \mathcal{N}_n} (x_n - x_m) [1 + |x_n - x_m|^{r_1-2}] = 0, \quad (45)$$

where \mathcal{N}_n denotes the set of nearest neighbours of lattice site n . Then, following (42) and (43), no energy threshold is present for $r_1 = 3$, whereas for the choice of $r_1 = 4$ a threshold is obtained. These predictions are confirmed by the numerical results for

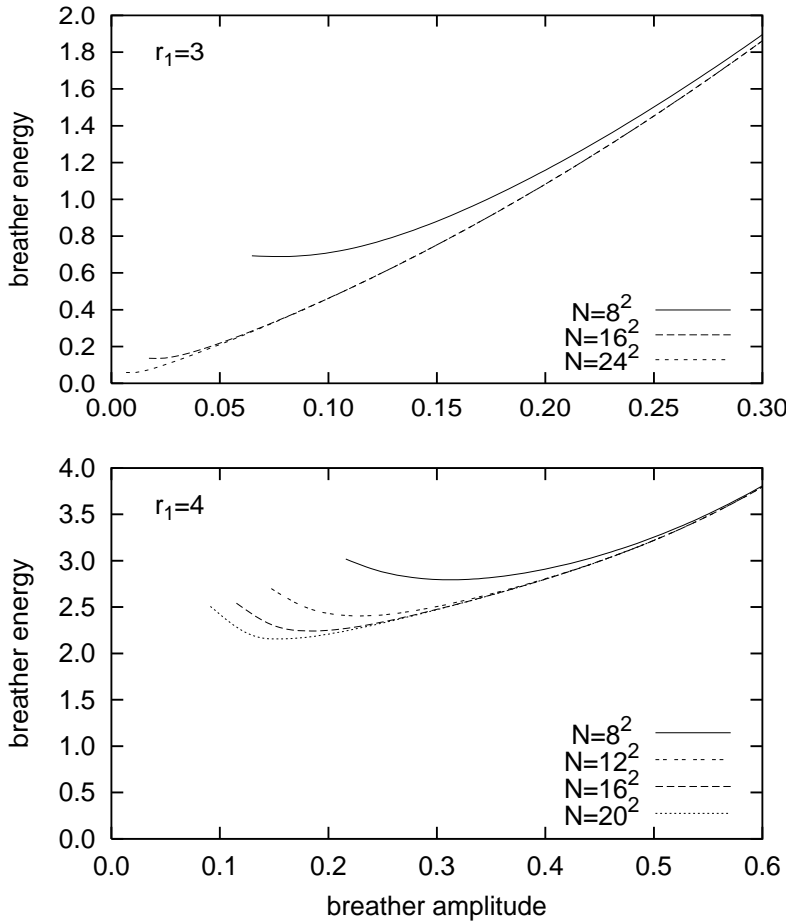


Figure 2. Breather energy versus amplitude for two-dimensional Fermi-Pasta-Ulam systems (45) with periodic boundary conditions for the cases $r_1 = 3$ and $r_1 = 4$. A lower bound on the breather energy is observed. For $r_1 = 3$, with increasing system size N this bound converges towards zero, whereas for $r_1 = 4$ it approaches a non-zero value.

finite systems with periodic boundary conditions presented in figure 2. For any finite number of lattice sites, a lower bound on the breather energy is observed. For $r_1 = 3$, with increasing system size N this bound converges towards zero, whereas for $r_1 = 4$ it approaches a non-zero value. Note that, for the system sizes considered, the range of validity of the large N approximation (38) has not yet been reached, as, in this approximation, no system size dependence of the energy threshold is expected in the case of $r_1 = 4$.

3.8. Generalizing to larger classes of systems?

The above result on energy thresholds for discrete breathers has been obtained for the class of systems defined in section 2. However, several of the restrictions have been imposed merely to keep the presentation clearer and for notational convenience, and we will discuss in the following which ones presumably could be removed.

It is obvious from (42) that the existence of an energy threshold is ruled by the power of the system size N in the expressions of the bifurcation energy (36) and (38). This power, in turn, can be traced back to the powers of the energy X in the series expansions of the frequency (15) of the band edge mode, and of the frequency (22) at which parametric resonance occurs. Although we have not explicitly done the calculations, we do not expect the powers in these expansions—and hence the energy thresholds for discrete breathers—to vary under a number of generalizations like

- other than hypercubic lattice geometries,
- states (p_n, x_n) with more than two components ($f > 1$ in the notation of section 2),
- interaction with a finite neighbourhood larger than nearest neighbours only,

Energy thresholds for discrete breathers in systems with Hamiltonian functions of other than the standard form (1), like the discrete nonlinear Schrödinger equation, have been considered in [15] and, on a rigorous level (i.e., without invoking our hypothesis 1), in [27]. Systems with asymmetric V and W are discussed in [23] for the case of analytic potentials. There it is found that allowing for asymmetric contributions in the series expansions (3) changes the expression for the bifurcation energy E_c , but it does not change the critical dimension d_c , and we would assume the same to happen for nonanalytic potentials. What *can* be modified by the inclusion of an asymmetric term, however, is whether low amplitude breathers do or do not exist in a certain system, and this issue is discussed in the next section.

For systems with long range interactions, the existence of energy thresholds is investigated in [16]. There it is found that the presence of long-range interactions enhances the appearance of an energy threshold, as shown for one-dimensional systems with analytic potentials, in which, in contrast to the short-range case, an energy threshold is observed.

3.9. Systems without low amplitude breathers

The above analysis leading to our result on energy thresholds for discrete breathers is heavily relying on the hypothesis stated in section 3.1, where it is assumed that breathers of arbitrarily low amplitude A_{DB} exist. This condition is fulfilled in many cases, but exceptions not only do exist, but they even appear to be generic. The class of systems without low amplitude breathers is defined by the property

$$\lim_{\omega_{\text{DB}} \rightarrow \omega_{\text{edge}}} A_{\text{DB}}(\omega_{\text{DB}}) \neq 0 \quad (46)$$

for all families of discrete breather present in the system when the breather frequency ω_{DB} approaches the frequency ω_{edge} of any of the band edge modes. First we want to give an example of a system without low amplitude breathers and study its characteristics. As a second step, some speculations are made on the general conditions leading to the absence of low amplitude breathers.

Consider a Fermi-Pasta-Ulam (FPU) chain, defined by Hamiltonian (2) with

$$V = 0 \quad \text{and} \quad W(x) = \frac{1}{2}x^2 + \frac{a}{3}x^3 + \frac{1}{4}x^4, \quad (47)$$

which gives rise to the equations of motion

$$\ddot{x}_n + \sum_{m=n\pm 1} [(x_n - x_m) + a(x_n - x_m)^2 + (x_n - x_m)^3] = 0. \quad (48)$$

For this system, two rigorous proofs of the existence of discrete breathers have been published. The first one is due to Aubry, Kopidakis and Kadelburg [4], using a variational method. These authors proof existence of discrete breathers for any strictly convex interaction potential W , which corresponds to a parameter a with $|a| < \sqrt{3}$ in (48). A second proof, applying a method of centre manifold reduction, was obtained by James [5], where existence of discrete breathers has been shown for values of a obeying $|a| < \frac{1}{2}\sqrt{3}$. Furthermore, as this latter method guarantees to catch all small amplitude solutions present in the system, the existence of small amplitude breathers can be excluded for $|a| > \frac{1}{2}\sqrt{3}$. Recapitulating, for the FPU chain (48) and parameter values $\frac{1}{2}\sqrt{3} < a < \sqrt{3}$, existence of discrete breathers can be proofed, but small amplitude breathers in the sense of (11) are clearly absent. Knowing that low amplitude breathers do not exist, it is a triviality to infer the existence of an energy threshold for discrete breathers.

To illustrate this result, numerical data, obtained by the continuation method described in section 3.7, are presented. The two cases $a = 0.4 < \frac{1}{2}\sqrt{3}$ and $\frac{1}{2}\sqrt{3} < a = 1.2 < \sqrt{3}$ are considered, which allows to confront the behaviour of systems with and without low amplitude breathers. Varying the breather frequency ω_{DB} and approaching the band edge of the linear spectrum, the breather amplitude at the site of maximum amplitude is monitored. The result is presented in figure 3, showing the amplitude to converge towards zero for $\omega_{\text{DB}} \rightarrow 2$ in the first case ($a = 0.4$), whereas a non-zero value is approached in this limit for the second case ($a = 1.2$).

Some speculations can be made regarding the general conditions under which exclusively large amplitude breathers (46) are observed, implying the existence of an energy threshold for discrete breathers. At the end of section 3.3 we noticed already that, for a tangent bifurcation of the band edge mode to take place in the class of systems considered, the expansion coefficients of the potentials (3) have to fulfill the inequalities (37) and (39) for the in-phase and the out-of-phase mode, respectively. For the FPU system (48), the corresponding inequality was already obtained in [23], equation (3.24), yielding $a \leq \frac{1}{2}\sqrt{3}$ in our notation. This inequality obviously coincides with the one deduced from the rigorous results [4] and [5], identifying the values of a providing low amplitude breathers. From this observation, one might deduce the following

HYPOTHESIS 2 *If, in a system with linear spectrum, no tangent bifurcation of any of the band edge modes take place, then discrete breathers of low amplitude in the sense of (11) do not exist.*

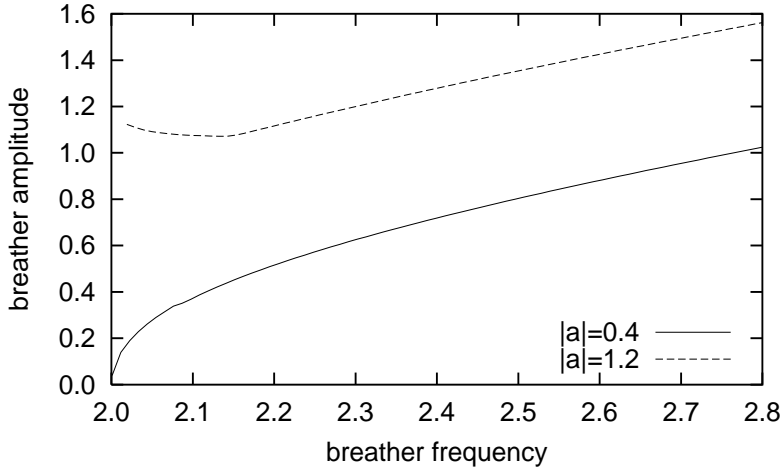


Figure 3. Breather amplitude versus frequency for system (48) with $N = 99$ lattice sites, free boundary conditions, and frequencies close to the band edge of the linear spectrum (which is at frequency 2.0). With parameter value $|a| = 0.4 < \frac{1}{2}\sqrt{3}$, breathers of arbitrarily low amplitude are observed, whereas for $\frac{1}{2}\sqrt{3} < |a| = 1.2 < \sqrt{3}$ the breather amplitude, and hence the breather energy, does not tend to zero when approaching the band edge of the linear spectrum.

This hypothesis, if correct, allows to deduce the existence of an energy threshold for discrete breathers from the mere absence of a tangent bifurcation of the band edge modes.

4. Systems with no linear spectrum

In analogy to the definition at the beginning of section 3, by the expression “systems with no linear spectrum” we want to refer to systems whose potential functions V and/or W of the Hamiltonian (1) are not quadratic in leading order. In the notation of the expansions in (3) this means simply $r_0 \neq 2$. The peculiar properties of such systems have attracted much interest recently, and strongly nonlinear tunable phononic crystals showing such a behaviour are currently being constructed [22].

In contrast to systems with linear spectrum where discrete breathers are known to be exponentially localized in space [1, 28], a localization even stronger than exponential is found in systems with no linear spectrum [28, 29, 30]. An upper bound on the breather amplitude is given by the inequality

$$|x_i| \leq a \exp(-|i|/b)c^{(d^i/3)} \quad (49)$$

for some $a, b, c, d \in \mathbb{R}$ in one-dimensional systems [30], where the breather is centred at site $i = 0$. However, arguments by which these results for the spatial decay can be obtained should be equally applicable in higher spatial dimension, and numerical computations confirm this reasoning, finding superexponential localization in higher dimensional systems.

Again, as in the preceding sections, we are interested in the low amplitude behaviour (if existing) of discrete breathers, which in turn affects the existence of an energy threshold. The mechanism as described in section 3, the emergence of discrete breathers from a bifurcation of a band edge plane wave, cannot take place here simply due to the absence of a linear spectrum. Nevertheless, it might in principle be the case that, when lowering the amplitude of a discrete breather in a system with no linear spectrum, the localization strength decreases, giving rise to an energy threshold in some spatial dimension. For lack of any better idea, some numerics was performed, suggesting for the (few) cases considered that

- (i) low amplitude breathers appear to exist, and
- (ii) the localization strength of discrete breathers remains constant in the low amplitude limit.

As an example, data are presented for a Klein-Gordon type system with Hamiltonian (1) and potentials

$$V(x) = \frac{1}{2}x^2 \quad \text{and} \quad W(x) = \frac{1}{3}|x|^3, \quad (50)$$

giving rise to the equations of motion

$$\ddot{x}_n = -x_n + \sum_{m \in \mathcal{N}_n} (x_m - x_n)|x_m - x_n|, \quad (51)$$

where \mathcal{N}_n denotes the set of nearest neighbours of lattice site n . Plotting the shape profiles of various discrete breathers obtained numerically for a one-dimensional system in figure 4, the above points (i) and (ii) are corroborated. Inspired by the numerical observations, we formulate the following

HYPOTHESIS 3 *Consider a system with no linear spectrum as specified above which supports discrete breathers. Then, low amplitude discrete breathers in the sense of (11) can be found. Furthermore, the localization strength is approximately constant within a family of discrete breathers.*

Note that this hypothesis is based only on numerical observations in a few examples of systems, both of FPU and Klein-Gordon type. From this hypothesis, the absence of an energy threshold for discrete breathers in arbitrary spatial dimension is deduced immediately. For illustration, numerical data are presented in figure 5 for system (51) in spatial dimensions $d = 1, 2, 3, 4$. Absence of an energy threshold is observed in any of these dimensions already for small finite systems. This is clearly distinct from the behaviour observed in figure 2 for systems with a linear spectrum where, if at all, the threshold vanishes in the limit of large system size only.

5. Summary of the results

We have studied the existence of energy thresholds for discrete breathers in a large class of Hamiltonian systems. Breather energies are found to have a positive lower bound if

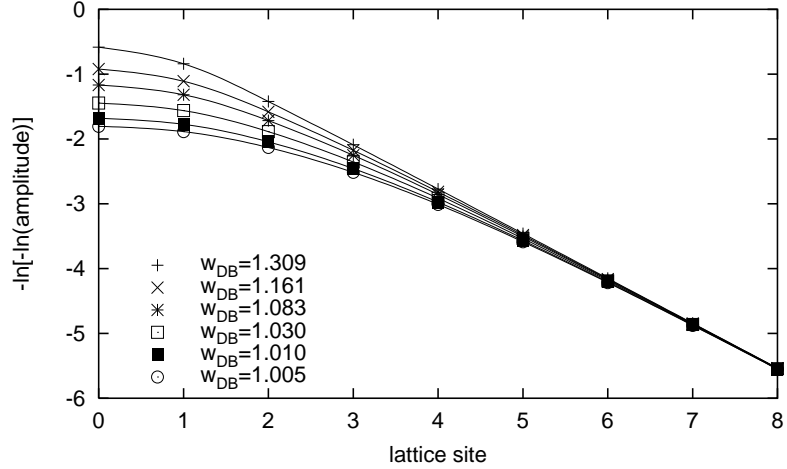


Figure 4. Shape profiles (maximum values of the amplitude) of discrete breathers, centered at site 0, in a system with no linear spectrum, namely the one-dimensional version of a Klein-Gordon type system with equations of motion (51) and $N = 99$ degrees of freedom. The localization strength is superexponential and remains unchanged when varying the maximum breather amplitude (or, equivalently, the breather frequency ω_{DB}). Note the twofold logarithmic scale of the ordinate ($-\ln[-\ln(\cdot)]$). Lines are merely drawn to guide the eye.

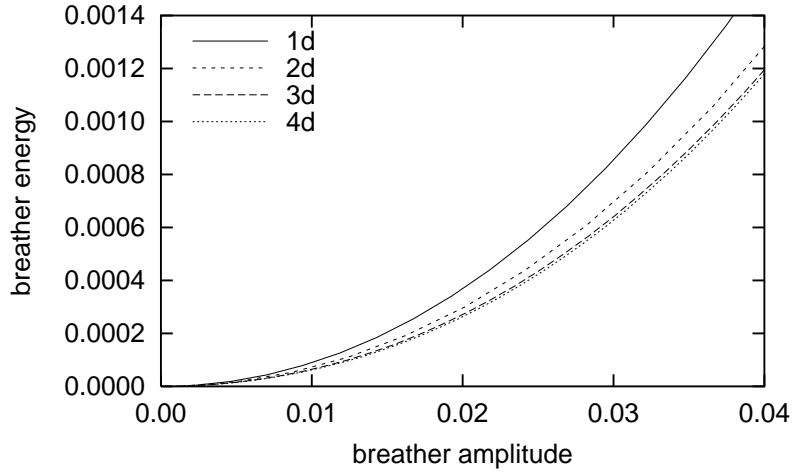


Figure 5. Energy versus amplitude for discrete breathers in a system with no linear spectrum. Independently of the spatial dimension $d = 1, 2, 3, 4$ (from top to bottom), arbitrarily low breather energies are observed. The data were obtained for systems consisting of $N = 8^d$ lattice sites, but, due to the strong (superexponential) localization, are indistinguishable on this scale from those of larger systems.

the lattice dimension d is greater than or equal to a certain critical value d_c , whereas no energy threshold is observed for $d < d_c$. The value of d_c depends on the class of systems under consideration, and we can distinguish the following three cases:

- (i) Systems with continuous linear spectrum which support low amplitude breathers: discrete breathers of low amplitude emerge from a tangent bifurcation of a band

edge mode. The bifurcation energy can be calculated explicitly and is related to a bound on the breather energy. For all finite systems, an energy threshold for discrete breathers is observed. For systems of large sizes N , this energy threshold scales as $N^{1-4/[d(r_1-2)]}$, resulting in a critical dimension $d_c = 4/(r_1 - 2)$ for infinite systems. (See section 2 for a definition of r_1 .)

- (ii) Systems with linear spectrum which do not support low amplitude breathers: no tangent bifurcation of a band edge mode is observed, and apparently no other mechanism for the creation of low amplitude breathers exist. As an immediate consequence of the absence of low amplitude breathers, an energy threshold for discrete breathers exists for finite as well as infinite systems.
- (iii) Systems with no linear spectrum: the localization strength of discrete breathers does not vary significantly with the frequency, and strongly localized low amplitude breathers appear to exist. This brings about the absence of an energy threshold for discrete breathers for finite as well as infinite systems, i.e., $d_c = \infty$.

Note that the above results are derived on the basis of hypotheses 1 to 3 formulated in sections 3 and 4. The hypotheses are corroborated in part by analytical results, in part by numerical observations.

Acknowledgments

Helpful comments from and discussions with Jérôme Dorignac, Sergej Flach and Roberto Livi are gratefully acknowledged. Thanks to Oliver Schnetz for readily providing mathematical support. This work was done during my stay at the Università di Firenze, Italy, in the group of Roberto Livi, supported by EU contract HPRN-CT-1999-00163 (LOCNET network).

References

- [1] MacKay R S and Aubry S 1994 Proof of existence of breathers for time-reversible or Hamiltonian networks of weakly coupled oscillators *Nonlinearity* **7** 1623–43
- [2] Bambusi D 1996 Exponential stability of breathers in Hamiltonian networks of weakly coupled oscillators *Nonlinearity* **9** 433–57
- [3] Livi R, Spicci M and MacKay R S 1997 Breathers on a diatomic FPU chain *Nonlinearity* **10** 1421–34
- [4] Aubry S, Kopidakis G and Kadelburg V 2001 Variational proof for hard discrete breathers in some classes of Hamiltonian dynamical systems *Discrete Contin. Dynam. Systems B* **1** 271–98
- [5] James G 2001 Existence of breathers on FPU lattices *C. R. Acad. Sci. Paris Sér. I Math.* **332** 581–6
- [6] James G 2003 Centre manifold reduction for quasilinear discrete systems *J. Nonlinear Sci.* **13** 27–63
- [7] James G and Noble P 2003 Breathers on diatomic FPU chains with arbitrary masses, in *Localization & Energy Transfer in Nonlinear Systems* ed Vázquez *et al* (Singapore: World Scientific) pp 225–32

- [8] Swanson B I, Brozik J A, Love S P, Strouse G F, Shreve A P, Bishop A R, Wang W-Z and Salkola M I 1999 Observation of intrinsically localized modes in a discrete low-dimensional material *Phys. Rev. Lett.* **82** 3288–91
- [9] Schwarz U T, English L Q and Sievers A J 1999 Experimental generation and observation of intrinsic localized spin wave modes in an antiferromagnet *Phys. Rev. Lett.* **83** 223–6
- [10] Trías E, Mazo J J and Orlando T P 2000 Discrete breathers in nonlinear lattices: experimental detection in a Josephson array *Phys. Rev. Lett.* **84** 741–4
- [11] Binder P, Abraimov D, Ustinov A V, Flach S and Zolotaryuk Y 2000 Observation of breathers in Josephson ladders *Phys. Rev. Lett.* **84** 745–8
- [12] Edler J and Hamm P 2002 Self-trapping of the amide I band in a peptide model crystal *J. Chem. Phys.* **117** 2415–24
- [13] Mandelik D, Eisenberg H S, Silberberg Y, Morandotti R and Aitchison J S 2003 Observation of mutually-trapped multi-band optical breathers in waveguide arrays *Phys. Rev. Lett.* **90** 253902
- [14] Sato M, Hubbard E, English L Q, Sievers A J, Ilic B, Czaplewski D A and Craighead H G 2003 Study of intrinsic localized vibrational modes in micromechanical oscillator arrays *Chaos* **13** 702–15
- [15] Flach S, Kladko K and MacKay R S 1997 Energy thresholds for discrete breathers in one-, two-, and three-dimensional lattices *Phys. Rev. Lett.* **78** 1207–10
- [16] Flach S 1998 Breathers on lattices with long range interaction *Phys. Rev. E* **58** R4116–9
- [17] Dorignac J and Flach S (unpublished)
- [18] Piazza F, Lepri S and Livi R 2003 Cooling nonlinear lattices toward energy localization *Chaos* **13** 637–45
- [19] Eleftheriou M, Flach S and Tsironis G P 2003 Breathers in one-dimensional nonlinear thermalized lattice with an energy gap *Physica D* **186** 20–6
- [20] Kastner M 2003 Energy thresholds for discrete breathers *Phys. Rev. Lett.* **92** 104301
- [21] Nesterenko V F 2001 *Dynamics of Heterogeneous Materials* (Berlin: Springer)
- [22] Nesterenko V F private communication
- [23] Flach S 1996 Tangent bifurcation of band edge plane waves, dynamical symmetry breaking and vibrational localization *Physica D* **91** 223–43
- [24] Nayfeh A H 1981 *Introduction to perturbation techniques* (New York: Wiley)
- [25] Magnus W and Winkler S 1966 *Hill's equation* (New York: Wiley)
- [26] Marín J L and Aubry S 1996 Breathers in nonlinear lattices: numerical calculation from the anticontinuous limit *Nonlinearity* **9** 1501–28
- [27] Weinstein M I 1999 Excitation thresholds for nonlinear localized modes on lattices *Nonlinearity* **12** 673–91
- [28] Flach S 1994 Conditions on the existence of localized excitations in nonlinear discrete systems *Phys. Rev. E* **50** 3134–42
- [29] Dey B, Eleftheriou M, Flach S and Tsironis G P 2001 Shape profile of compactlike discrete breathers in nonlinear dispersive lattice systems *Phys. Rev. E* **65** 017601
- [30] Yuan X 2002 Construction of quasi-periodic breathers via KAM technique *Comm. Math. Phys.* **226** 61–100